

Absence of static phase separation in the high T_c cuprate $\text{YBa}_2\text{Cu}_3\text{O}_{6+y}$

J. Bobroff¹, H. Alloul¹, S. Ouazi¹, P. Mendels¹, A. Mahajan^{1*}, N. Blanchard¹, G. Collin², V. Guillen³, J.-F. Marucco³

¹*Laboratoire de Physique des Solides, UMR 8502, Université Paris-Sud, 91405 Orsay, France*

²*LLB, CE-Saclay, CEA-CNRS, 91191 Gif sur Yvette, France*

³*LEMHE, UMR 8647, Université Paris-Sud, 91405 Orsay, France*
(December 2, 2024)

We use ^{89}Y NMR in $\text{YBa}_2\text{Cu}_3\text{O}_{6+y}$ in order to evaluate with high sensitivity the distribution of hole content p in the CuO_2 planes. For $y = 1$ and $y = 0.6$, this hole doping distribution is found narrow with a full width at half maximum smaller than $\Delta p = 0.025$. This rules out any large static phase separation between underdoped and optimally doped regions in contrast with the one observed by STM in Bi2212 and by NQR in LaSrCuO . This establishes that static electronic phase separation is not a generic feature of the cuprates.

In the cuprates, the hole doping of the CuO_2 planes induces the unusual features of the phase diagram: high- T_c superconductivity, strange metal behavior, pseudogap... A large body of theoretical work argues that this hole doping could be intrinsically strongly inhomogeneous in the planes, forming segregated hole-rich and hole-poor regions on a nanoscale [1]. This phase separation has been proposed to be essential to explain the unusual properties of the cuprates, appearing for example as stripes as argued from neutron scattering experiments [2]. Such proposals have been recently highlighted by STM studies which reveal strong inhomogeneities of the superconducting properties at the surface of Bi2212 [3] [4] [5] [6] [7]. Pan *et al.* have imaged a spatial distribution of the superconducting gap which they associated with a distribution of concentration of holes ranging from $p = 0.1$ to $p = 0.2$ holes/planar unit cell [5].

Deciding whether these electronic inhomogeneities exist in $\text{YBa}_2\text{Cu}_3\text{O}_{6+y}$ (YBaCuO), the archetype of the cuprate families as well would then elucidate if these inhomogeneities are only specific to some compounds and related to disorder. However, STM measurements are not as extensive in YBaCuO due to surface cleaving problems and oxygen loss in vacuum. The existing STM studies display an inhomogeneous or relatively homogeneous surface depending on the surface preparation procedure [8] [9]. These limitations do not occur if one uses other local probes such as nuclear magnetic (NMR) or quadrupolar resonance (NQR). The huge body of NMR/NQR studies done so far concentrated on the p -variation of the *average values* of specific quantities (i.e. the static NMR shift K or the relaxation time T_1). However, as will be emphasized hereafter, the NMR/NQR spectroscopy also allows to determine the distribution of these quantities in the *bulk* samples. NMR is then sensitive to the local distribution of electronic properties like STM, but not to the specificities of the surface. As an appealing example, Singer *et al* [10] evidenced recently a distribution of T_1 over the Cu NQR spectrum in bulk LaSrCuO , which can be attributed to a distribution of p as large as the one

observed on the Bi2212 surface.

We present an NMR static study of the YBaCuO family using ^{89}Y NMR spectra. This allows us to estimate the shape of the hole distribution in the bulk of the compound. We study two doping compositions (underdoped $\text{O}_{6.6}$ and slightly overdoped O_7). At O_7 the oxygen chains reservoirs are full, thus well ordered. At $\text{O}_{6.6}$, the various properties are weakly oxygen content dependent. So both compositions should produce a minimal disorder of doping in the planes. We show indeed that our results reveal a very narrow hole distribution. These results will be compared with other experiments in the various cuprate families.

We synthesized a large sample batch of single crystal grains of YBaCuO . It was oxidized at $T = 350^\circ\text{C}$, and then slowly cooled under oxygen atmosphere from 350°C to 270°C at a rate of 0.4K/hr . This procedure allows to reach the nominal maximum oxygen content $y = 1$ with a reduced $T_c = 89.1\text{ K}$ with respect to optimal doping ($T_c = 92.5\text{K}$). A part of this batch was reduced to $y = 0.60 \pm 0.02$ ($T_c = 55.8\text{K}$) under primary vacuum ($P = 0.13\text{ mbar}$) at $T = 385^\circ\text{C}$. The oxygen content was measured by thermogravimetry, i.e. measurement of weight loss during the deoxidisation process until equilibrium is reached in the above conditions. For both samples, the crystallites were then aligned in stycast epoxy in the field $H_{ext} (\simeq 7.5\text{ Tesla})$ of the NMR spectrometer. This field corresponds to a reference NMR resonance $^{89}\nu = 15634.67\text{ kHz}$ for a liquid YCl_3 solution. Spectra were obtained for H_{ext} perpendicular to the c cristallographic axis using a standard $\pi/2 - \pi$ pulse sequence and Fourier transform of half of the spin echo [11]. The repetition time of the pulse sequence was long enough at each temperature to recover the saturation signal for any value of p . For a given T , the maximum of $T_1(p)$ varies from 17 to 110 sec when decreasing T from 300K down to 120K .

^{89}Y NMR probes sensitively any doping distribution in the CuO_2 planes because the Y nucleus is coupled to Cu of its adjacent CuO_2 planes through the oxygen orbitals

[12]. This results in a shift of the NMR line related to the Cu spin susceptibility χ given by

$$^{89}\text{K}(T) = \frac{8A_{hf}\chi(T)}{\mu_B} + ^{89}\delta \quad (1)$$

Here, $^{89}\text{K}(T)$ is strongly dependent on hole content because of the strong hole doping dependence of $\chi(T)$. In contrast, the T -independent chemical shift $^{89}\delta$ and hyperfine coupling $A_{hf} = -1.95 \text{ kOe}/\mu_B$ between the ^{89}Y and one Cu do not change much with hole doping (μ_B is the Bohr magneton) [12]. This relation is illustrated in Fig.1 which displays the shift of the peak value of the ^{89}Y NMR line. It has been taken for a series of samples prepared from a single batch for different y . The shift $^{89}\text{K}(T)$ displays the well known behaviour for $\chi(T)$. It is nearly constant above optimal doping. It displays a marked decrease at low T which is the signature of the pseudogap for the underdoped cases. The oxygen content y can be converted into the hole content per plane using the parabolic dependence of T_c [13] given by $p = 0.16 \pm \sqrt{(1 - T_c/T_c^{\text{max}})/82.6}$. The corresponding p and experimental T_c are plotted in the inset of fig.1. Note that near optimal doping, the large p dependence of ^{89}K makes it a sensitive probe to any doping variation: for example, at $T = 120 \text{ K}$, a change in p as small as 0.01 corresponds to a change in ^{89}K of about 20 ppm, easily detectable. In the underdoped regime, the sensitivity to the doping is smaller but still sizeable.

The NMR spectrum of a given sample consists of a histogram of the NMR shifts throughout the sample. Note that, as STM, the NMR local probe is sensitive to variations nearly on the atomic scale, as each Y nucleus is coupled only to its 8 near neighbour Cu sites. Then, from the correspondence shift-doping of fig.1, any local distribution of doping will lead to a similar distribution in the shift, hence to a broadening of the spectrum.

Let us now present the experimental ^{89}Y NMR spectra for $y = 0.6$ and 1 from which we will extract quantitatively the actual doping distribution. The spectra are plotted for $T = 120\text{K}$ and 300K for the optimally and underdoped samples in fig.2. As can be observed immediately there is no significant overlap between the two spectra at $T = 120\text{K}$. This already proves that the O_7 ($p = 0.18$) sample contains no appreciable amount of underdoped nanoscale regions (equivalent to $p = 0.1$) and vice versa. In fig. 2 we also display the hole doping scales deduced from the relation between p and ^{89}K obtained from fig.1. From these hole doping scales it can be seen roughly that the full width at half maximum FWHM of the doping distribution is necessarily smaller than $\Delta p \simeq 0.04$ at optimal doping and 0.02 for the underdoped case. This clearly proves without any further analysis that the observed doping distribution in YBaCuO is much smaller than in Bi2212 and LSCO where $\Delta p \simeq 0.1$.

For a more quantitative analysis, we need to consider also that apart the distribution of $\chi(T)$, some unavoidable structural disorder yields local distributions of the

chemical shift δ and hyperfine coupling A_{hf} which enter Eq.1. These distributions are fully responsible for the FWHM $\Delta K = 32 \pm 5 \text{ ppm}$ of the undoped compound for $T > T_N$ [14]. Indeed, for oxygen content $y < 0.15$, no hole distribution broadening is expected [15]. This results from the fact that oxygens introduced in the Cu reservoir layer mainly convert the two adjacent $3d^{10} \text{ Cu}(1)$ into $3d^9$ and do not yield any hole doping of the CuO_2 planes, so that p is strictly 0. It is confirmed by the fact that the spectrum has the narrowest width among all dopings and is not found significantly dependent on oxygen content up to $y = 0.15$.

For higher y , if $\Delta\delta$ and ΔA_{hf} are the FWHM of the respective distributions assumed to be uncorrelated and gaussian for simplicity, this will lead to an additional broadening with FWHM $\Delta K(y, T)$:

$$\Delta K^2(y, T) = \Delta\delta^2(y) + \Delta K_{hf}^2(y, T) \quad (2)$$

where $\Delta K_{hf} = 8\mu_B^{-1} \Delta A_{hf} \chi(T)$. We note that the $y = 0$ compound is the more ordered as it is tetragonal with no twin boundaries and empty chains, hence $\Delta\delta$ and ΔA_{hf} should increase at higher y . As these broadenings add to the doping induced broadening, taking their $y = 0$ estimates at higher dopings will lead to an *overestimate* of the doping distribution. As ΔK_{hf} is T -dependent, we can evaluate ΔA_{hf} and $\Delta\delta$ separately. Indeed, at $y = 0.6$, $\chi(T)$ doubles between 120K and 300K so that ΔK_{hf} doubles as well, whereas the FWHM increases only by 11% as seen in fig.2. As this T -dependence might as well be due to the doping distribution, this leads to an upper bound $\Delta A_{hf}/A_{hf} \leq 0.13$. Such an upper bound would be explained in a naive hybridization computation by a random displacement of Cu by 0.04 \AA from its ideal position, a typical value from Rietveld measurements. We will consider the two extreme cases:

- (i) $\Delta A_{hf}/A_{hf} = 0$ corresponding to $\Delta\delta = 32 \text{ ppm}$
- (ii) $\Delta A_{hf}/A_{hf} = 0.13$ corresponding to $\Delta\delta = 29 \text{ ppm}$.

In order to extract the actual doping distribution, we start from a distribution of oxygen doping $P(y)$. We convert it for different temperatures into a shift distribution through the phenomenological ^{89}K vs y variation deduced from Fig.1. We convolute this K distribution with the δ and A_{hf} gaussian distributions with FWHM either (i) or (ii). This process is iterated until an optimal $P(y)$ is found to fit the experimental spectra for all temperatures with no additional free parameter.

In the underdoped $y = 0.6$ compound, this fitting procedure is limited by the fact that the NMR shift is nearly insensitive to the doping distribution for $y < 0.6$ as seen in fig.1. However, the thermogravimetry procedure during deoxydation constrains the measure of the average oxygen level $\bar{y} = 0.60 \pm 0.02$. We thus assume $P(y)$ to be symmetric around \bar{y} . The best fit is then obtained for a gaussian distribution $P(y) = \exp(-(y - 0.6)^2/\sigma^2)$ with $\sigma = 0.05$ for (i) and $\sigma = 0.1$ for (ii). This oxygen distribution $P(y)$ and the corresponding hole distribution $\mathcal{P}(p)$ are plotted in fig.3 together with the usual T_c di-

agram. The corresponding simulations fit perfectly the experimental ones at all temperatures (examples of fits are given as dotted lines in fig.2).

For YBaCuO₇, the chains are completely full. Further oxidation is prohibited. Therefore the distribution $P(y)$ is expected to be non symmetric [16]. To take this limitation into account, we model $P(y)$ as a convolution of a gaussian by $\exp(-|y-1|/\lambda_{\pm})$ where λ_{\pm} are allowed to differ for $y > 1$ and $y < 1$. The best fit is found for $\sigma = 0.01$, $\lambda_- = 0.06$, and $\lambda_+ = 0.025$ (i) or 0.004 (ii). $P(y)$ and the corresponding fit of the spectra are respectively plotted in fig.3 and fig.2. The high asymmetric shape towards $y < 1$ found for $P(y)$ confirms that no large overdoping of the planes is produced locally, as expected. In order to illustrate the high accuracy of our method, we choose $P(y)$ slightly broader than our best fit, plotted as the dotted line in the upper panel of fig.3. The corresponding simulation plotted as a dashed line in the upper panel of fig.2 clearly fails to fit the experimental spectrum.

In summary, our results demonstrate that the maximum possible distribution of doping is quite sharp with typical width $\Delta p \leq 0.025$ for optimal doping and $\Delta p \leq 0.01$ for the underdoped sample. The distribution is much smaller than in the LaSrCuO and Bi2212 cuprates. In LaSrCuO, at optimal doping, Singer *et al.* find $\Delta p \simeq 0.09$ as figured by the arrow in fig.3 [10]. Another NMR study [17] using ¹⁷O and ⁶³Cu NMR allowed to evidence a short length scale spatial modulation in underdoped LaSrCuO compatible with Ref. [10]. In Bi2212, the STM experiments reveal regions on the surface with the usual superconducting gap while others display a pseudogap [3] [4] [5] [6] [7]. This has been interpreted to be due either to some disorder effect [4] or to superconducting and insulating-like underdoped regions [5] [6] [7]. The corresponding doping distribution of width $\Delta p = 0.085$ extracted in Ref. [5] is plotted in fig.3. Similar widths are found for an optimally and an underdoped compound in Ref. [7]. Therefore, YBaCuO appears much more homogeneous than both LaSrCuO and Bi2212. In other cuprates, no key experiment was performed to probe locally the doping distribution, to our knowledge. However, in Hg1201 and Tl2201, typical ¹⁷O NMR widths are similar to those in YBaCuO and much smaller than in the Bi and La compounds [18]. Following the analysis done above and the proportionality between ¹⁷O and ⁸⁹Y shifts, we then expect the Hg and Tl family not to exhibit any strong doping distribution as well.

In the LaSrCuO family, the large distribution seen by NQR occurs in the bulk of the material and might be associated with tilt of the oxygen octaedra, buckling of the planes, stripes... In the Bi material, the STM results might be only a surface specificity. In YBaCuO, the doping distribution $P(y)$ measured here is not only much narrower but might even have only a macroscopic origin. As we used powders of cristallites with sizes smaller than 30 μm , any oxygen gradient within each cristallite, or a correlation between \bar{y} and the cristallite size could

lead to the observed $P(y)$. At O₇, such oxygen gradients are explained by the fact that oxygen diffusion between chains becomes limited at low temperature. This naturally leads to the asymmetry of $P(y)$ towards $y < 1$ seen in fig.3. This effect has been observed systematically in the various studies published by our group using ⁸⁹Y, or ¹⁷O NMR spectra in many different YBCO₇ powders. At O_{6.6}, the observed broad $P(y)$ is very narrow when plotted versus p (fig.3). Indeed a change in oxygen content does not strongly modify the actual hole doping of the planes near $y = 0.6$ hence leading to the plateau of T_c. This is to be associated with the fact that extra oxygens at such composition occupy empty chains, and do not modify the hole content, in analogy with the situation at $y = 0$. Therefore, the actual distributions would be much narrower on a submicron size region similar to the one sampled by STM. For both dopings, the key factor to the good homogeneity encountered is then probably the presence of the chains. The existing chain disorder does not lead to a sizeable distribution of hole content in the planes. Furthermore, those chains are probably sufficiently far from the planes not to stabilize a charge segregation. This specificity makes YBa₂Cu₃O_{6.6} or 7 some of the best prototypes of clean homogeneous cuprates.

In conclusion, the nanoscale static segregations observed so far cannot be considered as an intrinsic phenomenon common to all cuprates. The only remaining possibility for charge segregation or stripe-like scenario to apply in YBaCuO is then a dynamical process where the phase separation would have a lifetime smaller than our timescale of observation. For the present experiment, it corresponds to the inverse spectral width, typically 1 msec. Such dynamics might have been detected in inelastic neutron scattering experiments, but the existing results are still under debate [19] [20].

*present adress : Dept of Physics, IIT Bombay 400076 India.

-
- [1] V.J. Emery, S.A. Kivelson, H.Q. Lin, Phys. Rev. Lett. **64**, 475 (1990); J. Zaanen, O. Gunnarsson, Phys. Rev. Lett. **40**, 7391 (1989); V.J. Emery, and S.A. Kivelson, Physica C 209, 597 (1993).
 - [2] J. M. Tranquada *et al.*, Nature **375**, 561 (1995)
 - [3] J.-X. Liu *et al.*, Phys. Rev. Lett. **67**, 2195 (1991); A. Chang *et al.*, Phys. Rev. B **46**, 5692 (1992)
 - [4] T. Cren *et al.*, Phys. Rev. Lett. **84**, 147 (2000)
 - [5] S.H. Pan *et al.*, Nature, **413**, 282 (2001)
 - [6] C. Howald, P. Fournier, and A. Kapitulnik, Phys. Rev. B **64**, 100504 (2001)
 - [7] K.M. Lang *et al.*, Nature, **415**, 412 (2002)
 - [8] H.L. Edwards *et al.*, Phys. Rev. Lett. **75**, 1387 (1995)
 - [9] N.-C. Yeh *et al.*, Phys. Rev. Lett. **87**, 087003 (2001)
 - [10] P.M. Singer, A.W. Hunt and T. Imai, Phys. Rev. Lett.

88, 047602 (2002)

- [11] The orientation of the samples was chosen with H_{ext} perpendicular to the cristallographic c axis. In this direction, the spectra are weakly affected by the small fraction of non aligned polycrystallite grains present in the sample batch.
- [12] H.Alloul, T.Ohno and P.Mendels, Phys Rev.Lett. **63**, 1700 (1989)
- [13] J.L. Tallon *et al.*, Phys. Rev. B **51**, 12911 (1995)
- [14] H.Alloul *et al.*, Physica Amsterdam C **171**, 419 (1990)
- [15] The expected dipolar braodening from the nuclear Cu moments is an order of magnitude smaller than the observed linewidth.
- [16] We however allow for a small local doping distribution above $y = 1$. To do so in the following analysis, we extrapolate linearly the K values obtained between $y = 0.95$ and $y = 1$ up to $y = 1.1$, as observed in Hg compounds [18].
- [17] J. Haase *et al.*, Physica Amsterdam C **341-348**, 1727 (2000)
- [18] J. Bobroff *et al.*, Phys. Rev. Lett. **78**, 3757 (1997)
- [19] H.A. Mook and F. Dogan, Physica Amsterdam C **364-365**, 553 (2001)
- [20] P. Bourges *et al.*, Science **288**, 1234 (2000)

FIG. 1. ^{89}Y NMR shift ^{89}K for $H_{ext} \perp c$ for different *oxygen* contents y versus temperature. In the inset, T_c for each sample is plotted versus *hole doping* with the same symbol as the one used for K .

FIG. 2. ^{89}Y NMR Fourier Transform spectra are plotted at different temperatures and dopings in $\text{YBa}_2\text{Cu}_3\text{O}_{6+y}$ for $H_{ext} \perp c$ (black solid lines) with arbitrary normalization. In each panel, a doping scale gives the relation between the shift ^{89}K and hole doping p . Dotted lines are simulated spectra (see text). At $O_7:T=120\text{K}$, an additional dashed line is plotted, which corresponds to the simulation made using the dotted distribution of the upper panel of fig.3.

FIG. 3. The full black dots represent T_c versus oxygen content (upper panel) and hole doping (lower panel) for $\text{YBa}_2\text{Cu}_3\text{O}_{6+y}$. Distributions of oxygen content $P(y)$ and the corresponding distribution of hole content $\mathcal{P}(p)$ used to fit the spectra for $y = 1$ and $y = 0.6$ samples (see text). The dark and light gray enveloppes are obtained with a minimal distribution of chemical shift and hyperfine coupling within assumptions (i) and (ii) respectively. The dashed distribution and the arrow shown in the lower panel represent the distributions measured in Bi2212 [5] and LaSrCuO [10].

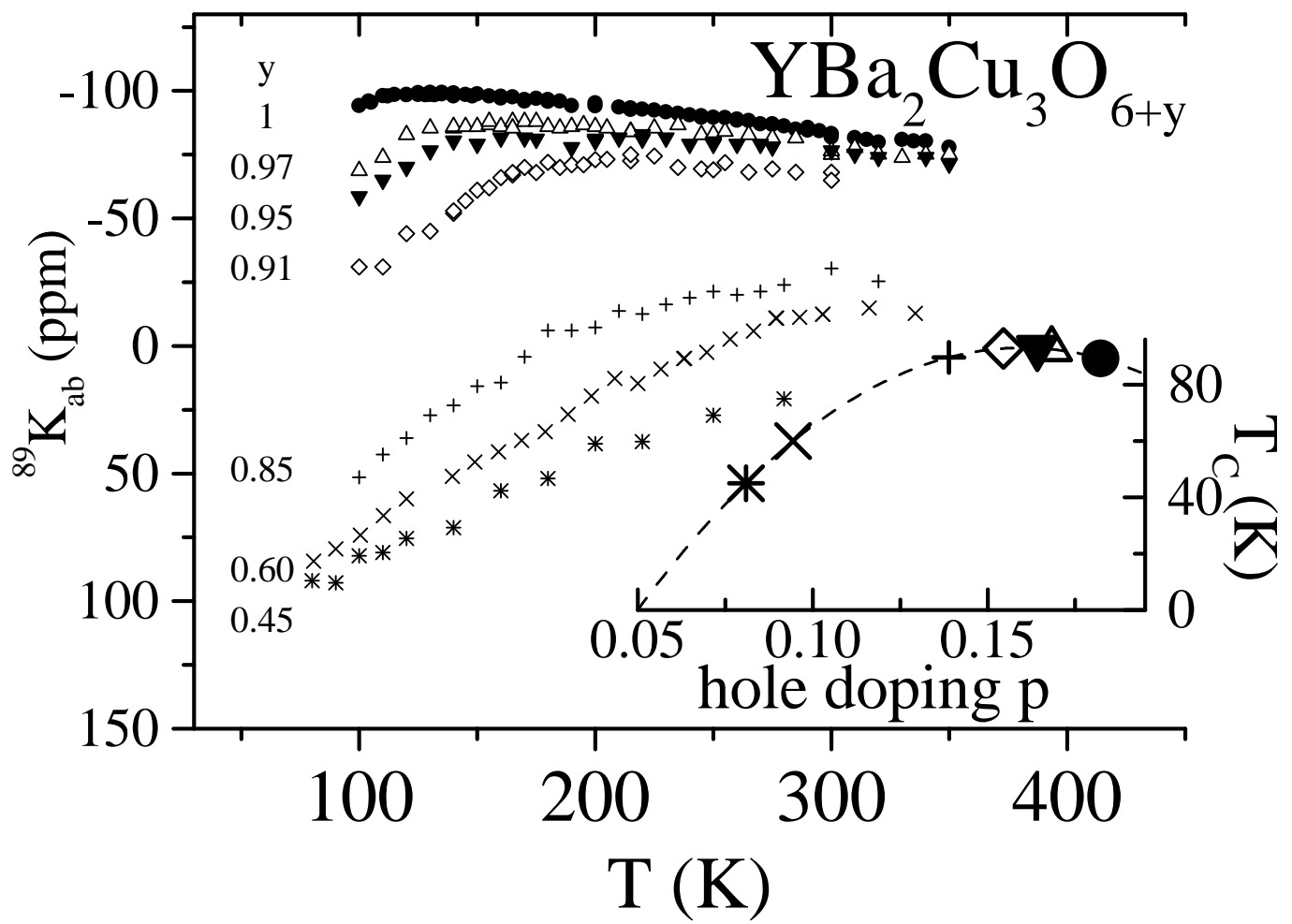


figure 1 (Bobroff et al. 2001)

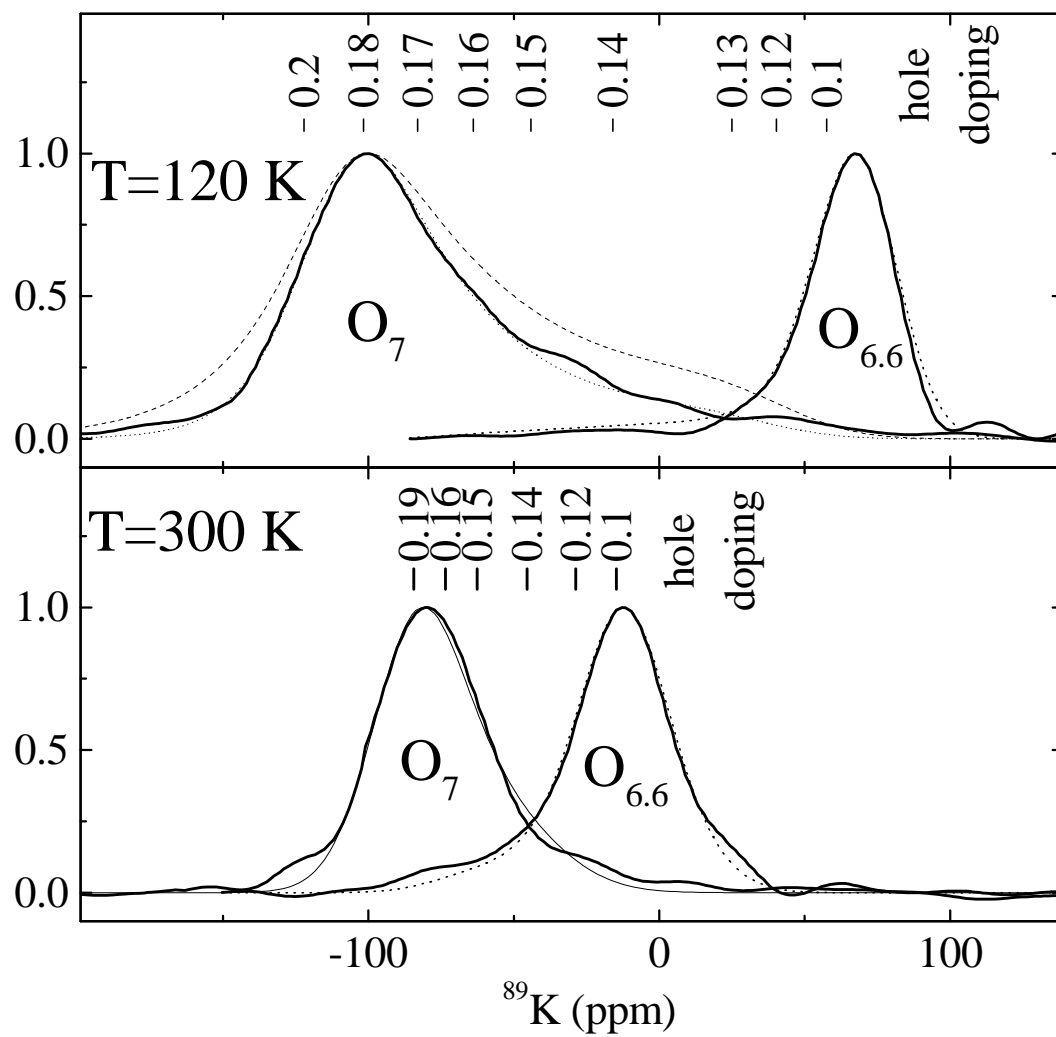


figure 2 (Bobroff et al. 2001)

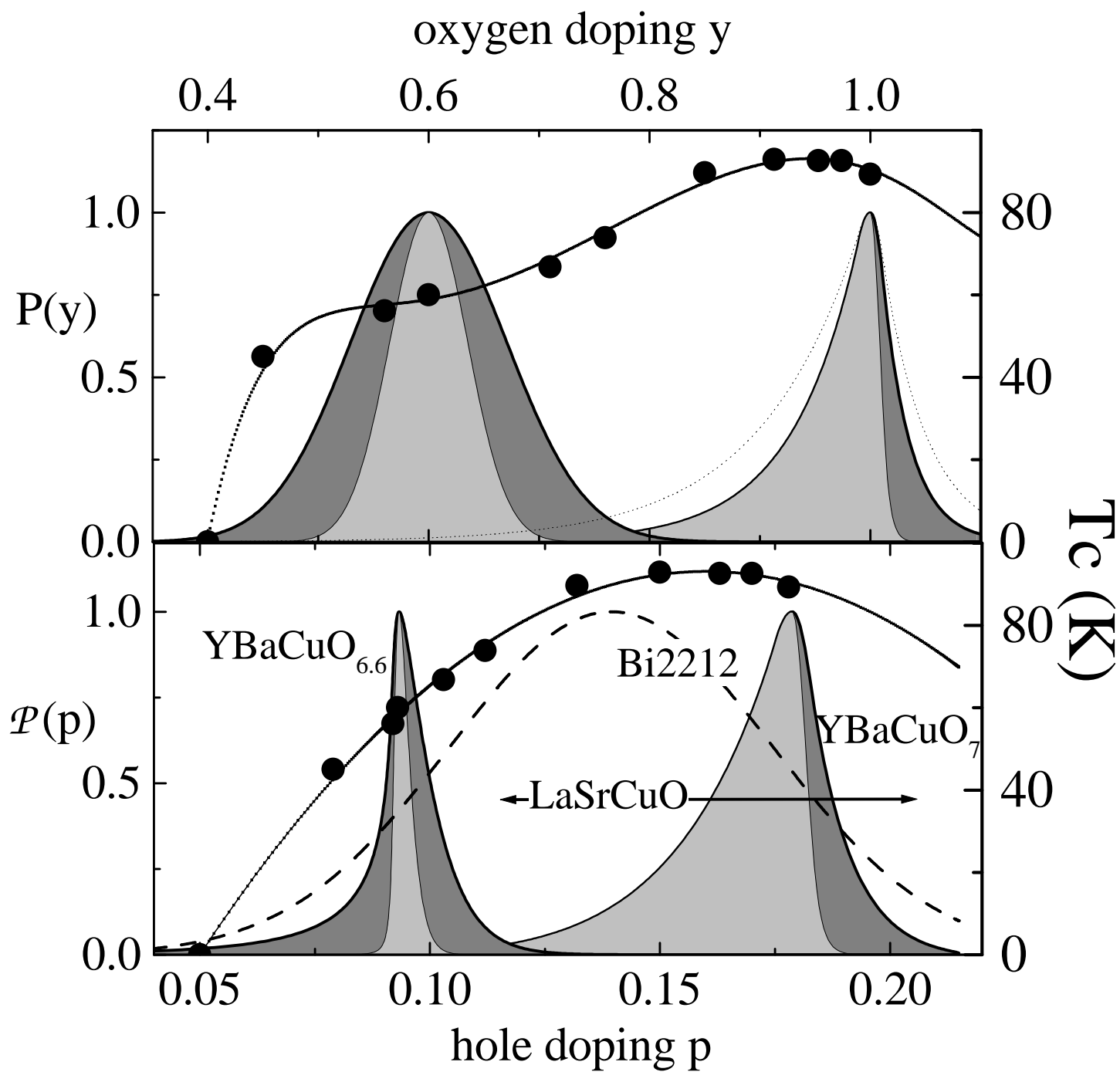


figure 3 (Bobroff et al. 2001)

